P-cluster maturation on nitrogenase MoFe protein

Yilin Hu, Aaron W. Fay, Chi Chung Lee, and Markus W. Ribbe*

Department of Molecular Biology and Biochemistry, University of California, Irvine, CA 92697

Communicated by Richard H. Holm, Harvard University, Cambridge, MA, May 8, 2007 (received for review February 28, 2007)

Biosynthesis of nitrogenase P-cluster has attracted considerable attention because it is biologically important and chemically unprecedented. Previous studies suggest that P-cluster is formed from a precursor consisting of paired [4Fe–4S]-like clusters and that P-cluster is assembled stepwise on MoFe protein, i.e., one cluster is assembled before the other. Here, we specifically tackle the assembly of the second P-cluster by combined biochemical and spectroscopic approaches. By using a P-cluster maturation assay that is based on purified components, we show that the maturation of the second P-cluster requires the concerted action of NifZ, Fe protein, and MgATP and that the action of NifZ is required before that of Fe protein/MgATP, suggesting that NifZ may act as a chaperone that facilitates the subsequent action of Fe protein/MgATP. Furthermore, we provide spectroscopic evidence that the [4Fe–4S] cluster-like fragments can be converted to P-clusters, thereby firmly establishing the physiological relevance of the previously identified P-cluster precursor.

assembly | NifZ

Nitrogenase provides the essential machinery for the biological reduction of dinitrogen to ammonia (for recent reviews, see refs. 1–5). The Mo-nitrogenase of *Azotobacter vinelandii* is a two-component system composed of the Fe protein and the MoFe protein. The homodimeric Fe protein has one ATP binding site per subunit and a single [4Fe–4S] cluster bridged in between the subunits, whereas the $\alpha_2\beta_2$-tetrameric MoFe protein (Fig. 1*A*) contains two unique clusters per $\alpha\beta$-subunit pair: the [8Fe–7S] P-cluster (6), which is located at the $\alpha\beta$-subunit interface, and the [Mo–7Fe–9S–X–homocitrate][†] iron–molybdenum cofactor (FeMoco) (7), which is positioned within the α-subunit. Nitrogenase catalysis involves a series of complex formation and dissociation between the Fe protein and the MoFe protein, during which process the electrons are sequentially transferred from the [4Fe–4S] cluster of the Fe protein, through the P-cluster, to the FeMoco within the MoFe protein, where substrate reduction eventually occurs. The complexity of nitrogenase reaction mechanism is undoubtedly associated with the presence of complex metalloclusters in the enzyme, namely, the P-cluster and FeMoco, the structure and function of which have served as one of the central topics in nitrogenase research for decades.

The P-cluster holds a unique place in nitrogenase chemistry. Catalytically, it serves as a "hub" that mediates the shuffling of electrons between the metal centers of the Fe protein and the MoFe protein. Structurally, it represents a high-nuclearity, Fe/S-only cluster that can be viewed as two [4Fe–4S] subclusters sharing a μ_6-sulfide. Such a "modular" composition suggests that the P-cluster is formed through the fusion of its substructural units, a reaction mechanism that is well established in synthetic inorganic chemistry (8) and further supported by recent advances toward successful synthesis of P-cluster topologs (9–12). Biological evidence of such a fusion mechanism came from studies of three FeMoco-deficient forms of *A. vinelandii* MoFe protein (Fig. 1*B*) that allowed analysis of P-cluster species without the interference of FeMoco. One of these MoFe proteins, designated Av1$^{\Delta nifH}$ (Fig. 1*B*, I), was obtained by deleting *nifH*, the gene encoding the subunit of Fe protein (13–16), whereas another of them, designated Av1$^{\Delta nifB}$ (Fig. 1*B*, III), was obtained by deleting *nifB*, the gene specifically involved in

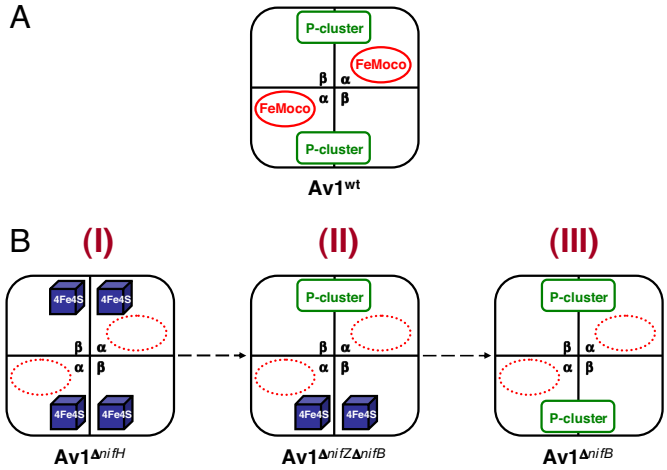

Fig. 1. Schematic representation of various forms of Av1. (*A*) Av1^{wt}, the wild-type form that contains a set of P-cluster and FeMoco in each $\alpha\beta$-dimer. (*B*) Av1$^{\Delta nifH}$ (I), a FeMoco-deficient form that contains a pair of [4Fe–4S]-like clusters in each $\alpha\beta$-dimer. Av1$^{\Delta nifZ\Delta nifB}$ (II), a FeMoco-deficient form that contains a P-cluster in one $\alpha\beta$-dimer and a pair of [4Fe–4S]-like clusters in the other. Av1$^{\Delta nifB}$ (III), a FeMoco-deficient form that contains a P-cluster in each $\alpha\beta$-dimer. Note that the paired [4Fe–4S] clusters in Av1$^{\Delta nifH}$ (I) and Av1$^{\Delta nifZ\Delta nifB}$ (II) presumably represent a precursor form of P-cluster during its assembly process.

FeMoco biosynthesis (17). Compared with Av1$^{\Delta nifB}$, which has two intact P-clusters (17), Av1$^{\Delta nifH}$ contains two pairs of [4Fe–4S]-like clusters in their places (14). Additionally, in contrast to Av1$^{\Delta nifB}$, which can be activated directly by isolated FeMoco (17), Av1$^{\Delta nifH}$ can be fully activated only after incubation with Fe protein and MgATP in crude extract (18). Thus, Av1$^{\Delta nifB}$ could represent the end product of P-cluster biosynthesis, whereas Av1$^{\Delta nifH}$ may represent a physiologically relevant intermediate that occurred at an earlier stage of this process. Apart from Av1$^{\Delta nifB}$ and Av1$^{\Delta nifH}$, a third form of FeMoco-deficient MoFe protein, designated Av1$^{\Delta nifZ\Delta nifB}$ (Fig. 1*B*, II), was obtained by deleting *nifZ*,[‡] the gene encoding a small protein with unknown function, along with *nifB* (19). Compared with the "all precursor" Av1$^{\Delta nifH}$ and the "all P-cluster" Av1$^{\Delta nifB}$, Av1$^{\Delta nifZ\Delta nifB}$ is a "half-assembled" form of MoFe protein, containing, in one $\alpha\beta$-subunit pair, a P-cluster, and in the other, a pair of [4Fe–4S]-like clusters (19). The [4Fe–4S]-like fragments in

Author contributions: Y.H. and M.W.R. designed research; Y.H., A.W.F., C.C.L., and M.W.R. performed research; Y.H. and M.W.R. analyzed data; and Y.H. and M.W.R. wrote the paper.

The authors declare no conflict of interest.

Abbreviation: FeMoco, iron–molybdenum cofactor.

*To whom correspondence should be addressed. E-mail: mribbe@uci.edu.

[†]The identity of X is unknown but is considered to be C, O, or N (7).

[‡]The MoFe protein resulting from deletion of *nifZ* alone, designated Av1$^{\Delta nifZ}$, has the same P-cluster composition as Av1$^{\Delta nifZ\Delta nifB}$, i.e., one P-cluster in one $\alpha\beta$-dimer and one pair of [4Fe–4S]-like clusters in the other, except that FeMoco is present in the $\alpha\beta$-dimer containing the fully assembled P-cluster.

This article contains supporting information online at www.pnas.org/cgi/content/full/0704297104/DC1.

www.pnas.org/cgi/doi/10.1073/pnas.0704297104

Table 1. Designations of proteins related to this work

Designation of protein	Genetic or biochemical handling	Source
$Av2^{wt}$	Wild-type Fe protein	*A. vinelandii* strain *Av*YM13A
$Av2^{E146D}$	E146D Fe protein point mutation	*A. vinelandii* strain *Av*YM48A
$Av2^{M156C}$	M156C Fe protein point mutation	*A. vinelandii* strain *Av*YM49A
$Av1^{wt}$	Wild-type MoFe protein	—
$Av1^{\Delta nifB}$	Histidine-tagged MoFe protein, deletion of *nifB gene*	*A. vinelandii* strain *Av*DJ1143
$Av1^{\Delta nifZ\Delta nifB}$	Histidine-tagged MoFe protein, deletion of *nifZ and nifB* genes	*A. vinelandii* strain *Av*YM6A
$Av1^{\Delta nifZ\Delta nifB}$(varied time)*		*A. vinelandii strain Av*YM6A
$Av1^{\Delta nifZ\Delta nifB}(0)$	$Av1^{\Delta nifZ\Delta nifB}$ was incubated 60 min without NifZ/$Av2^{wt}$/MgATP and subsequently repurified	—
$Av1^{\Delta nifZ\Delta nifB}$(15′, 30′, 45′, or 60′)	$Av1^{\Delta nifZ\Delta nifB}$ was incubated 15, 30, 45, or 60 min with NifZ/$Av2^{wt}$/MgATP and subsequently repurified	—
$Av1^{\Delta nifZ\Delta nifB}$(+Av2/ATP)*	$Av1^{\Delta nifZ\Delta nifB}$ was incubated 60 min with $Av2^{wt}$/MgATP and subsequently repurified	*A. vinelandii* strain *Av*YM6A
$Av1^{\Delta nifZ\Delta nifB}$(+NifZ)*	$Av1^{\Delta nifZ\Delta nifB}$ was incubated 60 min with NifZ and subsequently repurified	*A. vinelandii strain Av*YM6A
NifZ	Streptavidin-tagged NifZ	*E. coli* strain *Ec*YM1A

The component proteins of the Mo-nitrogenase are designated by the initials of the organism from which they are isolated and the Arabic numeral of the component. For example, MoFe protein and Fe protein of the Mo-nitrogenase of *A. vinelandii* are designated Av1 and Av2, respectively.
*Proteins were prepared as described in *Materials and Methods*.

$Av1^{\Delta nifZ\Delta nifB}$ are similar to those in $Av1^{\Delta nifH}$ (13–16, 19) (M. Cotton, K. Rupnik, R. Broach, Y.H., A.W.F., M.W.R., and B. J. Hales, unpublished work), indicating that $Av1^{\Delta nifZ\Delta nifB}$ may represent another physiologically relevant intermediate, midway in between the earlier intermediate represented by $Av1^{\Delta nifH}$ and the end product represented by $Av1^{\Delta nifB}$, during P-cluster assembly. Combined results from these studies suggest that (*i*) the final assembly of P-cluster occurs at its targeted location on the MoFe protein; (*ii*) the P-cluster is likely formed, *in vivo*, through fusion of small [4Fe–4S] cluster-like modules; (*iii*) the two P-clusters in the two $\alpha\beta$-subunit halves of the protein are assembled in a stepwise fashion; and (*iv*) Fe protein (*nifH* gene product) is required for P-cluster assembly in a process that involves MgATP hydrolysis; and (*v*) NifZ (*nifZ* gene product) is specifically involved in the formation of the "second" P-cluster.

Although a pair of [4Fe–4S]-like clusters has been associated with a P-cluster precursor under *in vivo* conditions, there is no direct proof that this precursor can indeed be converted to a mature P-cluster. In addition, the combinations of factors required for different stages of P-cluster assembly have not been determined. In this study, we specifically tackle the assembly process of the second P-cluster by combining biochemical and spectroscopic approaches. By using a P-cluster maturation assay that is based on purified components, we show that the maturation of the second P-cluster requires the concerted action of NifZ, Fe protein, and MgATP and that the action of NifZ is required before that of Fe protein/MgATP, suggesting that NifZ may act as a chaperone that facilitates the subsequent action of Fe protein/MgATP. Furthermore, we provide spectroscopic evidence that the [4Fe–4S] cluster-like fragments can be converted to P-clusters, thereby firmly establishing the physiological relevance of the previously identified P-cluster precursor.

Results

The various MoFe and Fe proteins in this work are designated Av1 and Av2, respectively, with appropriate superscripts defining the genetic background and/or biochemical handling of the proteins (e.g., the wild-type MoFe and Fe proteins are designated $Av1^{wt}$ and $Av2^{wt}$, respectively). For detailed designations, see Table 1.

Preparation of Components for P-Cluster Maturation. To establish the requirement for the maturation of the second P-cluster, the half-assembled $Av1^{\Delta nifZ\Delta nifB}$ and the factors known to be involved in P-cluster assembly, such as NifZ and $Av2^{wt}$, were prepared as follows. $Av1^{\Delta nifZ\Delta nifB}$ and $Av2^{wt}$ were homologously expressed in *A. vinelandii* and purified at yields of 200 and 400 mg per 200-g cell, respectively, whereas NifZ was heterologously expressed in *Escherichia coli* and isolated at a yield of 30 mg per 100-g cell. Purified NifZ is colorless. The polypeptide of NifZ is ≈19 kDa,[§] as shown by denaturing gel electrophoresis (Fig. 2*A*) and mass spectrometry (data not shown). Under native conditions, NifZ has an apparent molecular mass of ≈20 kDa (Fig. 2*B*), indicating that it is a monomeric protein.

Assessment of Requirement for P-Cluster Maturation. An *in vitro* P-cluster maturation assay was subsequently performed, in

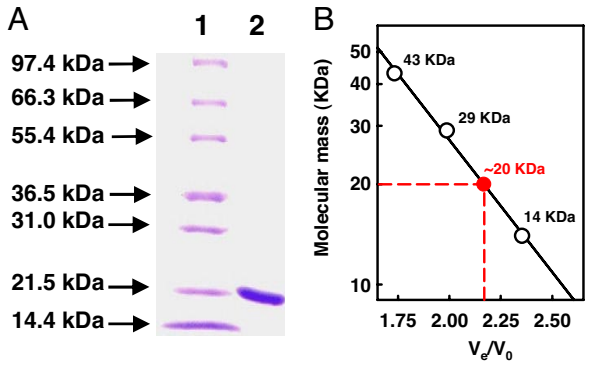

Fig. 2. Molecular mass determination of NifZ. (*A*) Coomassie blue-stained 10–20% gradient SDS/PAGE of purified, streptavidin-tagged NifZ. Lane 1, 10-μg protein standard; lane 2, 5-μg purified NifZ. The molecular mass of the polypeptide of streptavidin-tagged NifZ is ≈19 kDa, consistent with that determined by mass spectrometry (data not shown). (*B*) Determination of the native molecular mass of streptavidin-tagged NifZ by Ultrogel AcA 34 gel filtration (Pall Life Science, East Hills, NY). V_0, void volume; V_e, elution volume. Protein standards (white circles) are as follows: ribonuclease A (14 kDa), carbonic anhydrase (29 kDa), and ovalbumin (43 kDa). The apparent native molecular mass of streptavidin-tagged NifZ (red circle) is ≈20 kDa, suggesting a monomeric composition of the protein.

[§]The streptavidin-tagged NifZ has, in addition to the 160 amino acids from the NifZ sequence, 10 extra amino acids from the linker and streptavidin tag at the C terminus of the protein. Thus, the molecular mass of the subunit of streptavidin-tagged NifZ, theoretically calculated at 19.2 kDa, is slightly larger than that of nontagged NifZ.

Table 2. Determination of factors required for P-cluster maturation

	Assay components					Activities				
Line	Av1	NifZ	$Av2^{wt}$	ATP	FeMoco	C_2H_4 formation under C_2H_2/Ar	H_2 formation under Ar	NH_3 formation under N_2	H_2 formation under N_2	Average, %
1	$Av1^{\Delta nifB*}$	–	–	–	+	1,014 ± 29 (100)	998 ± 31 (100)	633 ± 6 (100)	223 ± 34 (100)	100
2	$Av1^{\Delta nifZ\Delta nifB\dagger}$	–	–	–	+	504 ± 4 (50)	545 ± 51 (55)	311 ± 7 (49)	108 ± 4 (48)	51
3	$Av1^{\Delta nifZ\Delta nifB}$	+	+	+	+	864 ± 33 (85)	888 ± 39 (89)	582 ± 22 (92)	173 ± 7 (78)	86
4	$Av1^{\Delta nifZ\Delta nifB}$	–	+	+	+	525 ± 6 (52)	576 ± 12 (58)	276 ± 50 (44)	118 ± 2 (53)	52
5	$Av1^{\Delta nifZ\Delta nifB}$	+	–	+	+	520 ± 8 (51)	550 ± 21 (55)	325 ± 51 (51)	105 ± 1 (47)	51
6	$Av1^{\Delta nifZ\Delta nifB}$	+	+	–	+	520 ± 42 (51)	567 ± 16 (57)	317 ± 52 (50)	113 ± 7 (51)	52
7	$Av1^{\Delta nifZ\Delta nifB}$	–	–	+	+	485 ± 7 (48)	545 ± 15 (55)	288 ± 54 (45)	110 ± 1 (49)	49
8	$Av1^{\Delta nifZ\Delta nifB}$	–	+	–	+	490 ± 17 (48)	559 ± 12 (56)	323 ± 50 (51)	111 ± 1 (50)	51
9	$Av1^{\Delta nifZ\Delta nifB}$	+	–	–	+	493 ± 15 (49)	537 ± 19 (54)	302 ± 58 (48)	111 ± 2 (50)	50

Activities of C_2H_4 formation under C_2H_2/Ar, H_2 formation under Ar, NH_3 formation under N_2, and H_2 formation under N_2 are expressed as nanomoles per minute per milligram of protein. Percentages relative to $Av1^{\Delta nifB}$ (line 1) are given in parentheses. The assays were performed as described in *Materials and Methods*. The lower detection limits for the activities were 0.01, 0.02, 0.001, and 0.02 nmol·min^{-1}·mg protein^{-1} for C_2H_4 formation under C_2H_2/Ar, H_2 formation under Ar, NH_3 formation under N_2, and H_2 formation under N_2, respectively.

*$Av1^{\Delta nifB}$ contains 100% fully assembled P-cluster and can be fully activated upon insertion of isolated FeMoco (17).

†$Av1^{\Delta nifZnifB}$ contains 50% fully assembled P-cluster and can be activated to 50% of that of $Av1^{\Delta nifB}$ in the absence of P-cluster maturation factors (19).

which $Av1^{\Delta nifZ\Delta nifB}$ was (*i*) incubated with combinations of NifZ, $Av2^{wt}$, and MgATP; (*ii*) activated by isolated FeMoco; and (*iii*) assayed for enzymatic activity. In the absence of maturation factors, $Av1^{\Delta nifZ\Delta nifB}$ (Table 2, line 2) can be activated to an average of 51% compared with $Av1^{\Delta nifB}$ (Table 2, line 1). This observation is consistent with the existing content of mature P-cluster, 50% and 100%, respectively, in $Av1^{\Delta nifZ\Delta nifB}$ and $Av1^{\Delta nifB}$ (Fig. 1*B*, II and III) (17, 19). Maturation of the second P-cluster in $Av1^{\Delta nifZ\Delta nifB}$, therefore, can be monitored by an increased activation that theoretically falls between the minimal 50% (one P-cluster per protein) and the maximal 100% (two P-clusters per protein).

As shown in Table 2, upon incubation with NifZ, $Av2^{wt}$, and MgATP, $Av1^{\Delta nifZ\Delta nifB}$ can be further activated to an average of 86% of the maximal level (Table 2, line 3), indicating a corresponding increase of the amount of mature P-cluster by 36%. Such an elevated level of $Av1^{\Delta nifZ\Delta nifB}$ reconstitution cannot be observed when one or two of these components are omitted (Table 2, lines 4–9). Thus, increased activation of $Av1^{\Delta nifZ\Delta nifB}$ involves the combined action of NifZ, $Av2^{wt}$, and MgATP. In the presence of excess MgATP, activation of $Av1^{\Delta nifZ\Delta nifB}$ reaches the empirical maxima at ≈2 μM NifZ (Fig. 3*A*) and ≈2.5 μM $Av2^{wt}$ (Fig. 3*B*). Given that $Av2^{wt}$ is the only known nucleotide-binding protein in the assay, it is mostly likely that $Av2^{wt}$-mediated hydrolysis of MgATP is required for this process. Indeed, when ATP is replaced by ADP or nonhydrolyzable analogues of ATP, such as 5′-adenylylimidodiphosphate or adenosine 5′-*O*-(3-thiotriphosphate) [supporting information (SI) Table 3, lines 3–5], $Av1^{\Delta nifZ\Delta nifB}$ cannot be activated beyond 50%. Furthermore, when $Av2^{wt}$ is replaced by $Av2^{M156C}$, an Av2 variant specifically defective in MgATP hydrolysis (20), no increased activation of $Av1^{\Delta nifZ\Delta nifB}$ is observed (SI Table 3, line 8), whereas, when $Av2^{wt}$ is replaced by $Av2^{E146D}$, an Av2 variant that supports normal MgATP hydrolysis despite being defective elsewhere (21), $Av1^{\Delta nifZ\Delta nifB}$ can still be activated to an average of 80% of the maximal level (SI Table 3, line 9).

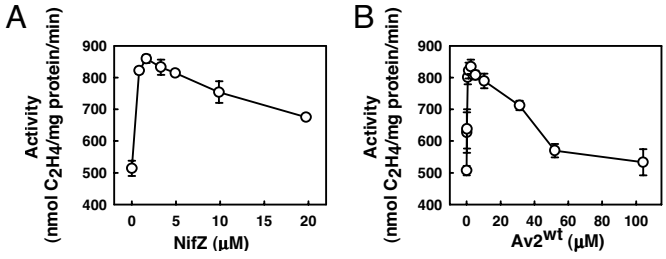

Fig. 3. Concentration-dependent P-cluster maturation on $Av1^{\Delta nifZ\Delta nifB}$. P-cluster maturation assays were performed as described in *Materials and Methods*, except that the concentration of NifZ was varied between 0 and 20 μM (*A*), and the concentration of $Av2^{wt}$ was varied between 0 and 104 μM (*B*). The maximal activities were reached at ≈2 μM NifZ (*A*) and 2.5 μM $Av2^{wt}$ (*B*), respectively. The data presented here represent the average of three independent experiments. The error bars are indicated.

Analysis of Cluster Conversion During P-Cluster Maturation. To obtain further evidence that the increased level of $Av1^{\Delta nifZ\Delta nifB}$ reconstitution is associated with the conversion of P-cluster precursor to mature P-cluster, a series of repurified $Av1^{\Delta nifZ\Delta nifB}$ proteins was obtained after incubation with NifZ, $Av2^{wt}$, and MgATP for increasing time intervals (categorically designated $Av1^{\Delta nifZ\Delta nifB/(varied\ time)}$; for detailed designations, see Table 1). Upon addition of isolated FeMoco, $Av1^{\Delta nifZ\Delta nifB(varied\ time)}$ proteins exhibit an increase in activation level that correlates with the increase in incubation time before repurification, reaching the maxima of 86% activation at 60 min (SI Table 4; also see Fig. 4*A*). When subjected to perpendicular-mode EPR analysis (Fig. 4*B*), dithionite-reduced $Av1^{\Delta nifZ\Delta nifB(varied\ time)}$ proteins show a decrease in the magnitude of the $S = ½$ signal that has been previously assigned to the P-cluster precursor in the "second half" of the $Av1^{\Delta nifZ\Delta nifB}$ protein (19), whereas, when subjected to parallel-mode EPR analysis (Fig. 4*C*), indigo disulfonate-oxidized $Av1^{\Delta nifZ\Delta nifB(varied\ time)}$ proteins display an increase in the intensity of the unique signal that is specific for the P-cluster in the P^{2+} oxidation state (22, 23), indicating an increase of mature P-cluster content as a result of the conversion of P-cluster precursor into fully assembled cluster. Over a time period of 60 min, the percentages of changes in perpendicular and parallel-mode EPR signals¶ are 32% and 41%, respectively, which correlate well with the 37% increase in activity (Fig. 4 and SI Table 4). $Av1^{\Delta nifZ\Delta nifB(varied\ time)}$ proteins also show an increase in

¶The percentages of changes of both perpendicular- and parallel-mode EPR signals of $Av1^{\Delta nifZ\Delta nifB(varied\ time)}$ were calculated by setting those of $Av1^{\Delta nifZ\Delta nifB(0)}$ as 50%, based on the fact that (*i*) the magnitude of the perpendicular-mode $S = ½$ signal of $Av1^{\Delta nifZ\Delta nifB(0)}$ represents the P-cluster precursor that can be converted to 50% of the total P-cluster content and (*ii*) the magnitude of the parallel-mode P^{2+} signal of $Av1^{\Delta nifZ\Delta nifB(0)}$ represents the existing P-cluster that accounts for 50% of the total P-cluster content.

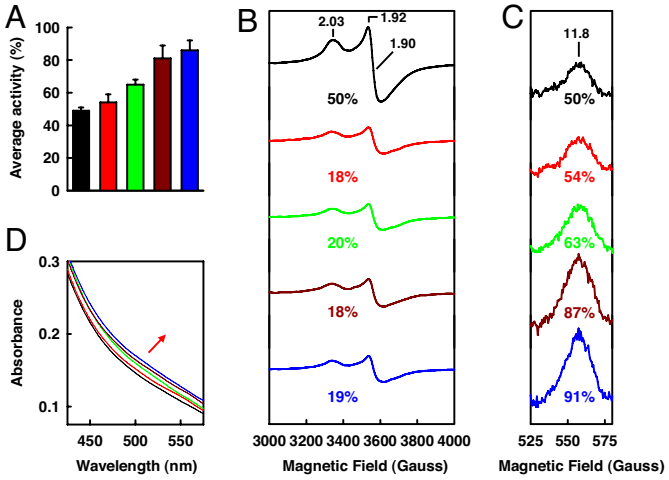

Fig. 4. Time-dependent P-cluster formation on Av1$^{\Delta nifZ\Delta nifB}$. Shown are average activities (*A*), perpendicular-mode EPR spectra (*B*), parallel-mode EPR spectra (*C*), and visible-range absorption spectra (*D*) of Av1$^{\Delta nifZ\Delta nifB(0)}$ (*A*, black bar; *B–D*, black lines), Av1$^{\Delta nifZ\Delta nifB(15')}$ (*A*, red bar; *B–D*, red lines), Av1$^{\Delta nifZ\Delta nifB(30')}$ (*A*, green bar; *B–D*, green lines), Av1$^{\Delta nifZ\Delta nifB(45')}$ (*A*, brown bar; *B–D*, brown lines), and Av1$^{\Delta nifZ\Delta nifB(60')}$ (*A*, blue bar; *B–D*, blue lines). EPR and visible-range absorption spectra were measured at protein concentrations of 10 and 5 mg/ml, respectively, as described in *Materials and Methods*. The time-dependent change of the visible-range absorption spectra during P-cluster maturation is indicated by the red arrow. The *g* values of the EPR spectra are indicated. The perpendicular (*B*) and parallel-mode EPR signals (*C*) are integrated as percentages of that of Av1$^{\Delta nifZ\Delta nifB(0)}$ (set as 50%).¶

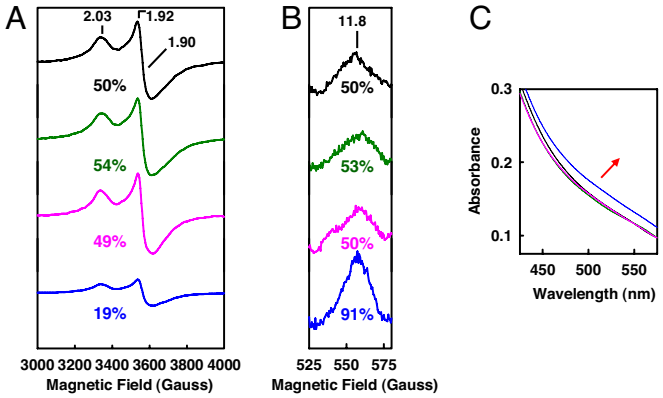

Fig. 5. Perpendicular-mode EPR spectra (*A*), parallel-mode EPR spectra (*B*), and visible-range absorption spectra (*C*) of Av1$^{\Delta nifZ\Delta nifB(0)}$ (black lines), Av1$^{\Delta nifZ\Delta nifB(+NifZ)}$ (green lines), Av1$^{\Delta nifZ\Delta nifB(+Av2/ATP)}$ (pink lines), and Av1$^{\Delta nifZ\Delta nifB(60')}$ (blue lines). EPR and visible-range absorption spectra were measured at protein concentrations of 10 and 5 mg/ml, respectively, as described in *Materials and Methods*. The time-dependent change of the visible-range absorption spectra during P-cluster maturation is indicated by the red arrow. The *g* values of the EPR spectra are indicated. The perpendicular (*B*) and parallel-mode EPR signals (*C*) are integrated as percentages of that of Av1$^{\Delta nifZ\Delta nifB(0)}$ (set as 50%).¶

the absorption intensity between 475 and 575 nm (Fig. 4*D*), a feature associated with an increase in the mature P-cluster content (15). It is interesting to note that, whereas the scale of precursor-associated $S = \frac{1}{2}$ signal cannot be reduced further with longer incubation (Fig. 4*B*), the magnitude of the P^{2+}-specific signal increases progressively with incubation time (Fig. 4*C*), which is consistent with the gradual increase in activity (Fig. 4*A*). These results suggest that the maturation of the P-cluster is likely a biphasic process, during which the initial modification of precursor occurs at a fast rate (within 15 min, Fig. 4*B*), whereas the eventual formation of P-cluster takes place at a slower pace (over 60 min) (Fig. 4*C*).

Determination of Sequence of Events of P-Cluster Maturation. To establish whether the actions of NifZ, Av2^{wt}, and MgATP occur in a sequential manner, repurified Av1$^{\Delta nifZ\Delta nifB}$ protein was produced after incubation with either NifZ alone [designated Av1$^{\Delta nifZ\Delta nifB(+NifZ)}$] or Av2^{wt} and MgATP [designated Av1$^{\Delta nifZ\Delta nifB(+Av2/ATP)}$] (for detailed designations, see Table 1). Neither Av1$^{\Delta nifZ\Delta nifB(+NifZ)}$ nor Av1$^{\Delta nifZ\Delta nifB(+Av2/ATP)}$ shows noticeable changes from Av1$^{\Delta nifZ\Delta nifB}$ in terms of spectroscopic properties (Fig. 5). Consistent with this observation, upon addition of isolated FeMoco, neither protein can be activated beyond 50% (SI Table 5, lines 2 and 5). Nevertheless, when combined with Av2^{wt} and MgATP, Av1$^{\Delta nifZ\Delta nifB(+NifZ)}$ protein can be activated to 85% (SI Table 5, line 7), whereas, combined with NifZ, Av1$^{\Delta nifZ\Delta nifB(+Av2/ATP)}$ cannot be activated above the baseline level of 50% (SI Table 5, line 3). These data strongly suggest that the maturation of P-cluster requires the action of NifZ before that of Av2^{wt}/MgATP and that the well-coordinated events carried out sequentially by NifZ and Av2^{wt}/MgATP initiate the modification of the precursor (Fig. 4*B*) that eventually leads to the formation of the mature P-cluster (Fig. 4*C*).

Discussion

Plausible Mechanism of P-Cluster Maturation. Our Av1$^{\Delta nifZ\Delta nifB}$-based studies of P-cluster maturation allow us to unambiguously identify the key factors for the assembly of the second P-cluster and, further, to establish the sequence of events during this process. More importantly, they provide direct spectroscopic proof (Fig. 4 *B–D*) that the P-cluster precursor, previously identified as paired [4Fe–4S]-like clusters (13–16, 19) (M. Cotton, K. Rupnik, R. Broach, Y.H., A.W.F., M.W.R., and B. J. Hales, unpublished work), can be converted to the mature P-cluster and, therefore, is indeed a physiologically relevant intermediate during the biosynthesis of P-cluster. With the physiological relevance firmly established for such a P-cluster precursor, a plausible stepwise mechanism of P-cluster biosynthesis could be proposed. As shown in Fig. 6, assembly of P-cluster on Av1 starts with two pairs of [4Fe–4S]-like clusters, one in each $\alpha\beta$-dimer of Av1 (represented by Av1$^{\Delta nifH}$). Upon combined action of Av2 and perhaps other unidentified factors, one pair of the [4Fe–4S]-like clusters is converted to a fully assembled P-cluster (represented by Av1$^{\Delta nifZ\Delta nifB}$). At this point, depending on the availability of FeMoco and the rate at which FeMoco is inserted, either the second pair of [4Fe–4S]-like clusters is converted to a P-cluster before the insertion of FeMoco (represented by Av1$^{\Delta nifB}$) or the FeMoco is inserted into the $\alpha\beta$-dimer containing the assembled P-cluster before the formation of the second P-cluster (represented by Av1$^{\Delta nifZ}$).‡‖ In either case, maturation of the second P-cluster is assisted by the concerted action of NifZ and Av2/MgATP, as well as some other factors that may further improve the efficiency of this process.

Role of NifZ in P-Cluster Maturation. Conversion of the second precursor starts with the action of NifZ, a small protein that exhibits little sequence homology to any other protein known to date.** Alone, NifZ does not alter the spectroscopic properties of the precursor (Fig. 5, green line). This observation, along with the primary sequence-based prediction that NifZ does not contain any defined metal- or metal cluster-binding motif,

‖Like Av1$^{\Delta nifZ\Delta nifB}$, Av1$^{\Delta nifZ}$ can be further activated upon incubation with NifZ, Av2^{wt}, and MgATP to a similar level (data not shown).

**Based on a sequence search using program BLAST (24), NifZ is widely distributed among bacterial organisms, such as Gram-positive bacteria, cyanobacteria, and purple bacteria. There is a highly conserved "NifZ domain," which consists of 75 amino acid residues at the N-terminal part of the protein.

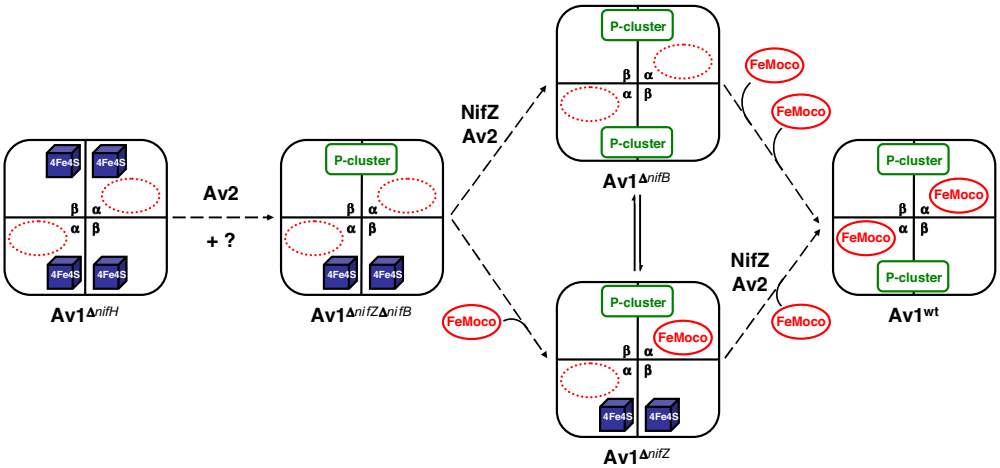

Fig. 6. Plausible mechanism of P-cluster maturation on Av1. Assembly of P-cluster on Av1 occurs stepwise, starting with two pairs of [4Fe–4S]-like clusters, one in each $\alpha\beta$-dimer of Av1 (represented by $Av1^{\Delta nifH}$). Upon the combined action of Av2 and perhaps other unknown factors, one pair of the [4Fe–4S]-like clusters is converted to a fully assembled P-cluster (represented by $Av1^{\Delta nifZ\Delta nifB}$). At this point, depending on the availability of FeMoco and the rate at which FeMoco is inserted, either the second pair of [4Fe–4S]-like clusters is converted to a P-cluster before the insertion of FeMoco (represented by $Av1^{\Delta nifB}$) or the FeMoco is inserted into the $\alpha\beta$-dimer containing the assembled P-cluster before the formation of the second P-cluster (represented by $Av1^{\Delta nifZ}$). In either case, maturation of the second P-cluster is assisted by the concerted action of NifZ and Av2/MgATP, as well as some other factors that may further improve the efficiency of this process.

indicates that NifZ does not function through a redox reaction. Interestingly, the action of $Av2^{wt}$/MgATP alone does not change the spectroscopic features of the precursor either (Fig. 5, pink line), and it is only after the task of NifZ is fulfilled that $Av2^{wt}$/MgATP can carry out its function by modifying the redox characteristics of the precursor that eventually results in the formation of mature P-cluster (Fig. 5, blue line; also see SI Table 5, line 7). It is possible, therefore, that NifZ acts as a chaperone by repositioning the precursor modules in a more favorable orientation for the redox action of $Av2^{wt}$/MgATP to take place.

Action of $Av2^{wt}$ in P-Cluster Maturation. The role of $Av2^{wt}$/MgATP in P-cluster biosynthesis has been implicated earlier by the observation that activation of $Av1^{\Delta nifH}$ requires the presence of both $Av2^{wt}$ and MgATP (15, 18). Furthermore, the all-precursor composition of $Av1^{\Delta nifH}$ (Fig. 1*B*, I) indicates that $Av2^{wt}$/MgATP also participates in an earlier step of P-cluster assembly that results in the formation of the "first" P-cluster. The absolute requirement of MgATP hydrolysis suggests that, like substrate reduction, P-cluster formation involves $Av2^{wt}$-mediated, MgATP hydrolysis-driven electron transfer; only in this case, the electrons are accepted by the P-cluster precursor instead of P-cluster. In support of this notion, redox changes of the precursor on the action of $Av2^{wt}$/MgATP have been observed in the cases of both $Av1^{\Delta nifZ\Delta nifB}$ (Fig. 4) and $Av1^{\Delta nifH}$ (15). Additionally, the significant conformational change of $Av2^{wt}$ upon MgATP hydrolysis could serve to bring the two [4Fe–4S] subclusters together in a process mimicking the docking of $Av2^{wt}$ on $Av1^{wt}$ during substrate reduction. However, P-cluster maturation occurs only at low concentrations of $Av2^{wt}$ and is inhibited by the presence of excess $Av2^{wt}$, where substrate reduction is not affected (Fig. 3*B*). This observation could be explained by limited accessibility of Av1 for NifZ at high concentrations of $Av2^{wt}$; or, alternatively, it could be explained by $Av2^{wt}$ using different mechanisms and/or different areas of the protein with different affinities for Av1 during P-cluster assembly and substrate reduction. Although essential for the assembly of both P-cluster and FeMoco, $Av2^{wt}$ apparently employs completely different parts of the protein for the two processes. This is based on the observation that $Av2^{E146D}$, an Av2 variant specifically defective in FeMoco biosynthesis, is fully competent in the P-cluster maturation assay (SI Table 3, line 9).

Closing Remarks. The fact that purified $Av1^{\Delta nifZ\Delta nifB}$ can be activated to 86% of the maximal level in the *in vitro* P-cluster maturation assay (Table 2, line 3) indicates that there may be other factors that further facilitate P-cluster assembly. These factors could be other *nif* gene-encoded products, such as NifW and NifM, which have been implicated in P-cluster assembly (25); or they could be other known chaperones, such as GroEL, which has been shown to participate in nitrogenase assembly (26). Our $Av1^{\Delta nifZ\Delta nifB}$-based assay could serve as a useful tool to identify other factors required for the maturation of the second P-cluster. Additionally, a similar assay can be developed on the basis of the all-precursor $Av1^{\Delta nifH}$, which will allow the identification of factors required for the assembly of the first P-cluster and the determination of the sequence of events in P-cluster biosynthesis within the MoFe protein (Fig. 6). Furthermore, the observation that the formation of P-cluster occurs in a relatively slow process could facilitate the time-dependent analysis of the conversion of P-cluster precursor to mature P-cluster and may allow us to eventually address the fate of the all-important "sulfur no. 8," the excess sulfur resulting from the fusion of the two [4Fe–4S] cluster modules during P-cluster formation.

Materials and Methods

Unless noted otherwise, all chemicals and reagents were obtained from Fisher (Hampton, NH), Aldrich (Milwaukee, WI), or Sigma (St. Louis, MO). For more details (13, 19, 20, 26–29), see *SI Methods*.

P-Cluster Maturation Assay. This assay (0.8 ml) contained 25 mM Tris·HCl (pH 8.0), 0.6 mg of purified $Av1^{\Delta nifZ\Delta nifB}$ (19), 0.03 mg of NifZ, 0.12 mg of $Av2^{wt}$, 20 mM $Na_2S_2O_4$, 0.8 mM ATP, 1.6 mM $MgCl_2$, 10 mM creatine phosphate, 8 units of creatine kinase, and 10 μl of isolated FeMoco. This mixture was then incubated at 30°C for 60 min and determined for enzymatic activities (26–29). Note that addition of excess $Av2^{wt}$ at this point completely inhibited P-cluster maturation on

$Av1^{\Delta nifZ\Delta nifB}$ (Fig. 3*B*) but had no effect on the subsequent activity assay.

P-Cluster Maturation Assay on $Av1^{\Delta nifZ\Delta nifB}$. This assay (25 ml) contained 25 mM Tris·HCl (pH 8.0), 100 mg of $Av1^{\Delta nifZ\Delta nifB}$, 5 mg of NifZ, 20 mg of $Av2^{wt}$, 2.4 mM ATP, 4.8 mM $MgCl_2$, 30 mM creatine phosphate, and 24 units/ml creatine kinase. The mixture was stirred at 30°C for 15, 30, 45, and 60 min, respectively, before $Av1^{\Delta nifZ\Delta nifB}$ was repurified [designated $Av1^{\Delta nifZ\Delta nifB(\text{varied time})}$]. Control $Av1^{\Delta nifZ\Delta nifB(0)}$ was prepared by omitting NifZ/$Av2^{wt}$/ATP. $Av1^{\Delta nifZ\Delta nifB(+\text{NifZ})}$ and $Av1^{\Delta nifZ\Delta nifB(+\text{Av2/ATP})}$ were prepared by omitting $Av2^{wt}$/ATP and NifZ, respectively.

This work was supported by National Institutes of Health Grant GM-67626 (to M.W.R.).

1. Burgess BK, Lowe DJ (1996) *Chem Rev* 96:2983–3011.
2. Howard JB, Rees DC (1996) *Chem Rev* 96:2965–2982.
3. Smith BE (1999) *Adv Inorg Chem* 47:159–218.
4. Rees DC, Tezcan FA, Haynes CA, Walton MY, Andrade S, Einsle O, Howard JB (2005) *Philos Trans R Soc London A* 363:971–984.
5. Peters JW, Szilagyi RK (2006) *Curr Opin Chem Biol* 10:1–8.
6. Peters JW, Stowell MHB, Soltis SM, Finnegan MG, Johnson MK, Rees DC (1997) *Biochemistry* 36:1181–1187.
7. Einsle O, Tezcan FA, Andrade SLA, Schmid B, Yoshida M, Howard JB, Rees DC (2002) *Science* 297:1696–1700.
8. Lee SC, Holm RH (2004) *Chem Rev* 104:1135–1158.
9. Berlinguette CP, Miyaji T, Zhang Y, Holm RH (2006) *Inorg Chem* 45:1997–2007.
10. Zhang Y, Holm RH (2004) *Inorg Chem* 43:674–682.
11. Zhang Y, Holm RH (2003) *J Am Chem Soc* 125:3910–3920.
12. Zuo JL, Zhou HC, Holm RH (2003) *Inorg Chem* 42:4624–4631.
13. Ribbe MW, Hu Y, Guo M, Schmid B, Burgess BK (2002) *J Biol Chem* 277:23469–23476.
14. Corbett MC, Hu Y, Naderi F, Ribbe MW, Hedman B, Hodgson KO (2004) *J Biol Chem* 279:28276–28282.
15. Hu Y, Corbett MC, Fay AW, Webber JA, Hedman B, Hodgson KO, Ribbe MW (2005) *Proc Natl Acad Sci USA* 102:13825–13830.
16. Broach RB, Rupnik K, Hu Y, Fay AW, Cotton M, Ribbe MW, Hales BJ (2006) *Biochemistry* 45:15039–15048.
17. Schmid B, Ribbe MW, Einsle O, Yoshida M, Thomas LM, Dean DR, Rees DC, Burgess BK (2002) *Science* 296:352–356.
18. Tal S, Chun TW, Gavini N, Burgess BK (1991) *J Biol Chem* 266:10654–10657.
19. Hu Y, Fay AW, Dos Santos PC, Naderi F, Ribbe MW (2004) *J Biol Chem* 279:54963–54971.
20. Bursey EH, Burgess BK (1998) *J Biol Chem* 273:29678–29685.
21. Ribbe MW, Bursey EH, Burgess BK (2000) *J Biol Chem* 275:17631–17638.
22. Pierik AJ, Wassink H, Haaker H, Hagen WR (1993) *Eur J Biochem* 212:51–61.
23. Tittsworth RC, Hales BJ (1993) *J Am Chem Soc* 115:9763–9767.
24. Altschul SF, Gish W, Miller W, Myers EW, Lipman DJ (1990) *J Mol Biol* 215:403–410.
25. White TC, Harris GS, Orme-Johnson WH (1992) *J Biol Chem* 267:24007–24016.
26. Ribbe MW, Burgess BK (2001) *Proc Natl Acad Sci USA* 98:5521–5525.
27. Burgess BK, Jacobs DB, Stiefel EI (1980) *Biochim Biophys Acta* 614:196–209.
28. Gavini N, Burgess BK (1992) *J Biol Chem* 267:21179–21186.
29. Corbin LJ (1984) *Appl Environ Microbiol* 47:1027–1030.